Implantation of Tetrapod-Shaped Granular Artificial Bones or β-Tricalcium Phosphate Granules in a Canine Large Bone-Defect Model

Sungjin CHOI[1,2]#, I-Li LIU[1]#, Kenichi YAMAMOTO[2], Muneki HONNAMI[1,3], Takamasa SAKAI[3], Shinsuke OHBA[2], Ryosuke ECHIGO[1], Shigeki SUZUKI[4], Ryouhei NISHIMURA[1], Ung-il CHUNG[2,3], Nobuo SASAKI[1] and Manabu MOCHIZUKI[1]*

[1]*Laboratory of Veterinary Surgery, Graduate School of Agricultural and Life Sciences, The University of Tokyo, 1–1–1 Yayoi, Bunkyo-ku, Tokyo 113–8657, Japan*
[2]*Center for Disease Biology and Integrative Medicine, Graduate School of Medicine, The University of Tokyo, 7–3–1 Hongo, Bunkyo-ku, Tokyo 113–0033, Japan*
[3]*Department of Bioengineering, School of Engineering, The University of Tokyo, 7–3–1 Hongo, Bunkyo-ku, Tokyo 113–0033, Japan*
[4]*NEXT21 K.K., 3–38–1 Hongo, Bunkyo-ku, Tokyo 113–0033, Japan*

ABSTRACT. We investigated biodegradability and new bone formation after implantation of tetrapod-shaped granular artificial bone (Tetrabone®) or β-tricalcium phosphate granules (β-TCP) in experimental critical-size defects in dogs, which were created through medial and lateral femoral condyles. The defect was packed with Tetrabone® (Tetrabone group) or β-TCP (β-TCP group) or received no implant (control group). Computed tomography (CT) was performed at 0, 4 and 8 weeks after implantation. Micro-CT and histological analysis were conducted to measure the non-osseous tissue rate and the area and distribution of new bone tissue in the defect at 8 weeks after implantation. On CT, β-TCP was gradually resorbed, while Tetrabone® showed minimal resorption at 8 weeks after implantation. On micro-CT, non-osseous tissue rate of the control group was significantly higher compared with the β-TCP and Tetrabone groups ($P<0.01$), and that of the β-TCP group was significantly higher compared with the Tetrabone group ($P<0.05$). On histology, area of new bone tissue of the β-TCP group was significantly greater than those of the Tetrabone and control groups ($P<0.05$), and new bone distribution of the Tetrabone group was significantly greater than those of the β-TCP and control groups ($P<0.05$). These results indicate differences in biodegradability and connectivity of intergranule pore structure between study samples. In conclusion, Tetrabone® may be superior for the repair of large bone defects in dogs.
KEY WORDS: artificial bones, β-TCP granules, canine, critical-size defect, Tetrabone.

doi: 10.1292/jvms.13-0054; *J. Vet. Med. Sci.* 76(2): 229–235, 2014

Large bone defects may be problematic, and bone grafts are frequently used to repair such defects. An autograft is an excellent scaffold for bone regeneration—it is easily incorporated into the host bone and contains abundant osteogenic cells, matrix and osteoinductive proteins [4]. However, use of an autograft has potential problems, including morbidity of the donor site, insufficient amount of bone graft that can be harvested and the requirement for additional surgery [1].

Currently, a large number of artificial bone alternatives are commercially available, and they vary in composition, mechanism of biological reaction and structural characteristics. Calcium phosphate, such as hydroxyapatite (HA) and tricalcium phosphate (TCP; subdivided into α- and β-TCP), has been widely used as artificial bone in orthopedic, maxillofacial and plastic surgery, because these materials show high biocompatibility and osteoconductivity [10]. However, HA has a low degradation rate and takes a long time to be replaced by new bone tissue *in vivo* [2, 5]. TCP is more commonly used, because of its biodegradability.

Porosity of artificial bone materials is an important factor in adhesion, proliferation and differentiation of osteogenic cells *in vitro* and *in vivo* [8, 9]. Furthermore, Yoshikawa *et al*. reported that connectivity is the primary determinant for osteoconductivity [18]. Therefore, development of artificial bone with adequate porous structure is required for an ideal bone graft.

We developed Tetrabone®, a novel tetrapod-shaped granular artificial bone, comprising a mixture of α-TCP and octacalcium phosphate (OCP) granules of homogeneous size [3]. The mixture generates highly connected intergranular pores between the Tetrabone® granules, which enhances invasion of blood vessels and osteogenic cells [3]. In our previous experiment, which used a rabbit bone defect model to clarify the long-term effects of Tetrabone® implantation, Tetrabone® showed synchronized resorption and new bone formation while maintaining mechanical strength throughout the observation period.

The purpose of this study was to investigate the *in vivo* effects of Tetrabone® implantation in large bone defects regarding biodegradability and new bone formation in dogs
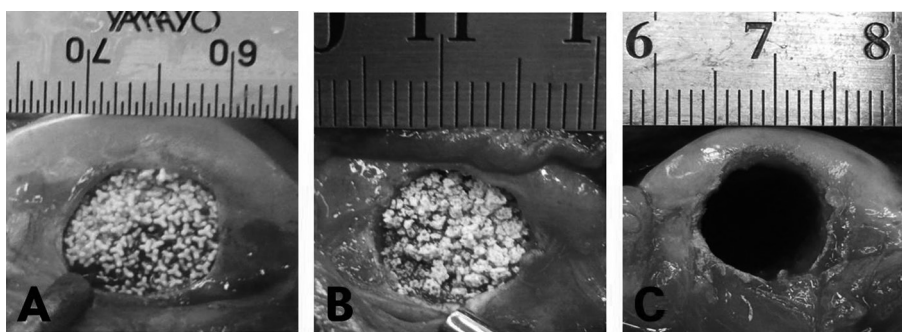
Fig. 1.   Defects with a diameter of 10 mm were created through the femoral condyles of dogs. Tetrabone (A) or β-TCP granules (B) were implanted. The defect was not filled in the control group (C).

and to compare the effects with those of β-TCP granules which are most widely used in clinics.

MATERIALS AND METHODS

Preparation of implants: The fabrication process of Tetrabone® has been described in a previous study [3]. Briefly, 60/40 vol% α-TCP powder (Taihei Chemical Industrial Co., Tokyo, Japan) and binder (a mixture of 55% olefin resin, 30% wax and 15% plasticizing materials) were mixed for 30 min, and then, wax and plasticizing materials were extensively mixed with the former materials at room temperature in a rotating-drum tumbler mixer (K03P, Neo Tecs, Osaka, Japan) for 4.5 hr. Tetrapod-shaped injection molds with a size of 1 mm were prepared, and the α-TCP compound was injected using an injection-molding machine (J35AD; Japan Steel Works, Tokyo, Japan). The molded products were degreased at a maximum temperature of 500°C for 1 hr and calcined at a maximum temperature of 700°C for 1 hr. After calcination, the products were soaked in 0.2 mol/*l* succinic acid for 24 hr to form OCP, rinsed with distillated water twice and dried under reduced pressure. Finally, the tetrapod-shape granular artificial bones 1 mm in size were obtained and sterilized by electron beam irradiation at 25 kGy. β-TCP granules (Osferion®; particle diameter, 0.5–1.5 mm; porosity, 75%) were purchased from Olympus Biomaterial Corporation (Tokyo, Japan).

Surgical procedures: Seven male beagle dogs, weighing 10–12 kg and aged 1–2 years, were purchased from Japan Laboratory Animals Inc. (Tokyo, Japan). All the experimental procedures using dogs were conducted according to the Guidelines of the Animal Care Committee of the Graduate School of Agricultural and Life Sciences, the University of Tokyo.

Preanesthetic medication consisted of subcutaneous (SC) injection of atropine sulfate (25 μg/kg) followed by intravenous (IV) injection of fentanyl hydrate (5 μg/kg). Anesthesia was induced with propofol (6 mg/kg IV) and maintained with 1.0–2.5% isoflurane and oxygen after tracheal intubation. Cefazolam (20 mg/kg IV) was injected as a preoperative antibiotic. For analgesia, administration of 5–20 μg/kg/hr fentanyl hydrate was started at the time of induction of

anesthesia and continued for 12 hr postoperatively.

Both femurs were clipped, aseptically prepared with povidone-iodine and draped for surgery. A longitudinal skin incision was made along the femoral axis over the medial femoral condyle and extended through the joint capsule. The joint capsule and patella ligament were carefully elevated over the proposed site of the defect, and the trochlea was exposed. A tunnel defect 10 mm in diameter was created from the medial to lateral condyle using a power surgery drill (IMEX™ Veterinary, Inc., Longvew, TX, U.S.A.), and bone debris was removed and flushed with sterile saline. For preparation of the implant, the end of a 2.5 m*l* syringe barrel was cut, and Tetrabone® (Tetrabone group) or β-TCP granules (β-TCP group) were packed with sterile saline. To minimize the dead space between the granules, they were packed using 24G needle. The same amount of granules to the defect volume packed with sterile saline was put into the defect, and the granules were gently packed with a bar (n=5 each group; Fig. 1A and 1B). Both openings of the defect were sealed with a fibrinogen adhesive (Bolheal®; Kaketsuken, Tokyo, Japan). Four defects were maintained without implantation (n=4; control group; Fig. 1C). The implant sites of 3 groups were set randomly. After implantation, the joint capsule, fascia lata and subcutaneous tissue were sutured in a continuous suture pattern with 3-0 or 4-0 polydioxanone, and the skin was closed in an interrupted pattern with 3-0 nylon. The same surgical procedure was performed in the contralateral femur of each subject, and all operative procedures were performed under sterile conditions.

For postoperative care, buprenorpine (15 μg/kg) by intramuscular (IM) injection and cefazolam (20 mg/kg SC) were injected twice a day for 3 days. Robert-Jones bandages were applied to both hind limbs for 7 days after surgery. All dogs were observed daily for any appearance of abnormal clinical signs.

Computed tomography (CT): CT was performed immediately after the surgery and at 4 and 8 weeks of implantation under sedation with midazolam (0.3 mg/kg IM) and medetomidine (20 μg/kg IM). CT data were converted to a transverse section of the defect using a DICOM image viewer (OsiriX; The Osirix Foundation, Geneva, Switzerland), and the changes in images of the implant sites were observed.

Gross evaluation: At 8 weeks of implantation, the dogs were euthanatized with rapid KCl injection under deep anesthesia with thiopental sodium. The implants and surrounding tissue of the defects were grossly observed, and the distal femurs were excised using a sagittal saw (Osada Electronics, Tokyo, Japan).

Micro-CT: Micro-CT of the femoral condyles was performed immediately after excision by using a micro-CT scanner (InspeXio; Shimadzu Science East Corporation, Tokyo, Japan) with a voxel size of 100 μm/pixel at 90 kV and 110 μA. For micro-CT analysis, transverse sections of the defects were reconstructed using image analyzing software (Tri/3D-Bon; RATOC System Engineering Co., Ltd., Tokyo, Japan). A region of interest (ROI) with a diameter of 10 mm and a height corresponding to that of the tunnel defect was placed on the micro-CT image. We masked the space having a lower intensity signal than that of bone in the ROI, and this space was defined as non-osseous tissue. The volume of the space was measured and expressed as a percentage of the whole defect area.

Histology: The excised femoral condyles were fixed in neutral 10% formalin (Wako, Tokyo, Japan) for 7 days and demineralized with Plank-Rychlo decalcifying solution (Wako, Tokyo, Japan) for 12 weeks. After decalcification, the specimen was longitudinally bisected at the middle of the trochlea into medial and lateral halves. The specimens were dehydrated in ascending grades of ethanol, embedded in paraffin, sliced in 7-μm transverse sections and stained with Masson's Trichrome. The stained sections were examined under a light microscope (Biozero; Keyence, Osaka, Japan) for the evaluation of new bone tissue.

We measured the area and the distribution of new bone tissue using image analyzing software (Image J; US National Institutes of Health, Bethesda, MD, U.S.A.). The margins of the bone tissues were measured manually at high magnification ($\times$ 40) on each single section. The area of new bone tissue indicated only the new bone tissue that had calcified matrix within the bone defect (Fig. 2A). The distribution of new bone tissue is defined as the inner area from the margin of the defect to the outer margin of the new bone (Fig. 2B). Each parameter was expressed as a percentage of the whole defect area.

Statistical analysis: Data are expressed as mean and standard deviation. Statistical analysis was performed using one-way analysis of variance (ANOVA) with a software program
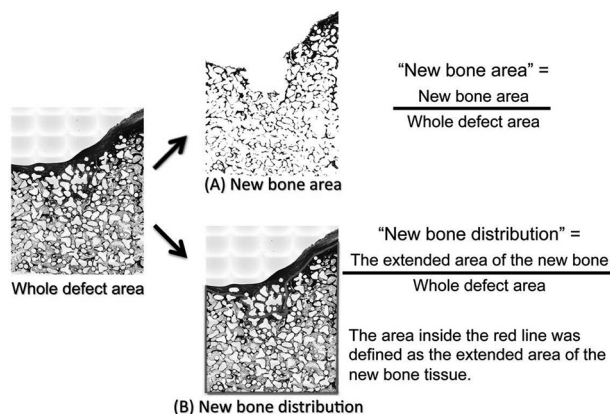

Fig. 2. The calculation methods of new bone area and (A) new bone distribution (B).

(Prism; GraphPad Software, Inc., La Jolla, CA, U.S.A.). The data were further analyzed by Tukey's post hoc multiple comparisons test. A *P* value less than 0.05 was considered statistically significant.

RESULTS

Gross evaluation: Figure 3 shows gross findings of the implanted site in each group at 8 weeks of implantation. There were no abnormal findings, such as inflammation or infection, in any of the groups. In the Tetrabone group, the granules completely filled the defect and were connected to the surrounding tissue. In the β-TCP and control groups, the granules were not grossly observed, and the opening of the defect was concave.

CT findings: Typical CT findings of the defect in each group at each time point are shown in Fig. 4. In the Tetrabone group, the quantity of granules and the appearance of the implanted site showed no changes up to 8 weeks of implantation. In the β-TCP group, resorption of granules was observed at both ends and the central area of the defect from 4 weeks of implantation. In the control group, a small amount of new bone tissue was observed within the defect at 4 and 8 weeks of implantation.

Micro-CT: Figure 5 shows the typical transverse micro-CT images in each group at 8 weeks of implantation. In the Tet-
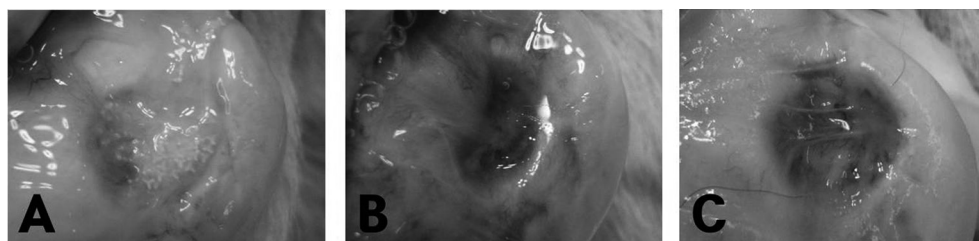

Fig. 3. Gross appearances of the implanted sites at 8 weeks of implantation. The granules filled the defect during the experimental periods in Tetrabone group (A), while β-TCP granules were not observed (B). The opening of the defect was concave in the β-TCP and control groups (B, C).
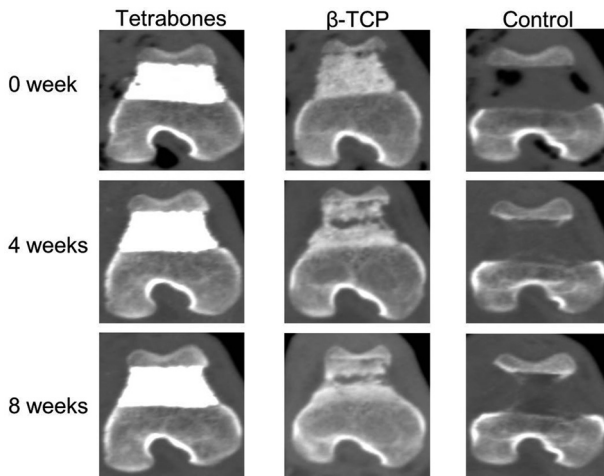
Fig. 4.   Transverse CT images of the defects in the 3 groups at 0, 4
and 8 weeks of implantation. In Tetrabone group, there were no
changes in images during the experimental period. In the β-TCP
group, the granules were already absorbed at 4 and 8 weeks of the
implantation. A small amount of new bone tissue was observed
within the defect at 4 and 8 weeks of implantaion

Fig. 5.   Transverse micro-CT images at 8 weeks of implantation. In
the Tetrabone group, intergranular pores appeared to be well con-
nected (A, B). In the β-TCP group, the granules at the bone ends
and the central area of the defects disappeared (C, D). A limited
volume of new bone was found in the control group (E, F).

rabone group, granules appeared to be well connected with
new bone formation between the granules within the defect
at 8 weeks of implantation. In the β-TCP group, resorption
resulted in granule loss at both ends and the central area of
the defect. In the surrounding area, minimal new bone tissue
was observed. In the control group, a limited volume of new
bone was found in the defect.

Figure 6 shows the non-osseous tissue rate on the micro-
CT images of each group at 8 weeks of implantation. The
non-osseous tissue rate was $19.95 \pm 5.18\%$ in the Tetrabone
group, $34.31 \pm 9.12\%$ in the β-TCP group and $90.40 \pm 3.15\%$
in the control group. The value of the control group was
significantly higher than those of the β-TCP and Tetrabone
groups ($P<0.01$), and that of the β-TCP group was signifi-
cantly higher than that of the Tetrabone group ($P<0.05$).

Histological observation: Figure 7 shows the typical his-
tological findings of the bisected transverse section in each
group. In the Tetrabone group, new bone tissue was found
in the intergranular spaces and was fully distributed in the
defect area. In the β-TCP group, both new bone and fibrous
tissues were found in the defect. There were no tissues in
the central area of the defect, leading to the appearance of
empty space. The new bone tissue in the β-TCP group was
partially distributed mainly adjacent to the original bone. In
the control group, a large amount of fibrous tissue was found
in the defect, with empty space at the center of the defect and
scant new bone tissue near the original bone.

Figure 8 shows the new bone area on the histological sec-
tion of each group. The new bone area was $10.32 \pm 0.75\%$ in
the Tetrabone group, $13.64 \pm 2.52\%$ in the β-TCP group and
$5.11 \pm 1.72\%$ in the control group. The value of the β-TCP
group was significantly higher than those of the Tetrabone
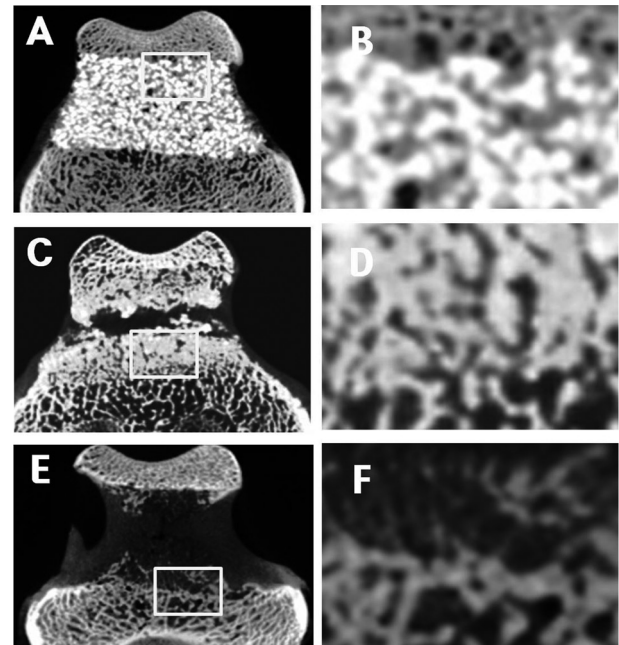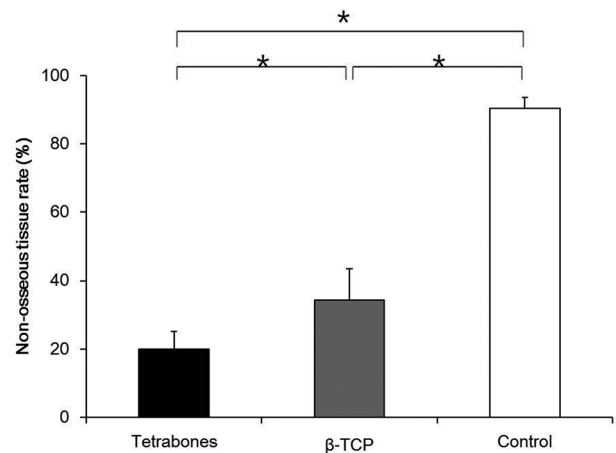and control groups ($P<0.05$), and that of Tetrabone group

Fig. 6.   Non-osseous tissue rate of the 3 groups. Non-osseous tissue
rate in the Tetrabones group was significantly lower than those in
the β-TCP and control groups ($P<0.05$).

was significantly higher than that of the control group
($P<0.05$).

The new bone distribution was $99.38 \pm 0.98\%$ in the Tet-
rabone group, $87.01 \pm 7.91\%$ in the β-TCP group and $79.17
\pm 15.61\%$ in the control group. The value of the Tetrabone
group was significantly higher than those of the β-TCP and
control groups ($P<0.05$). There was no significant difference
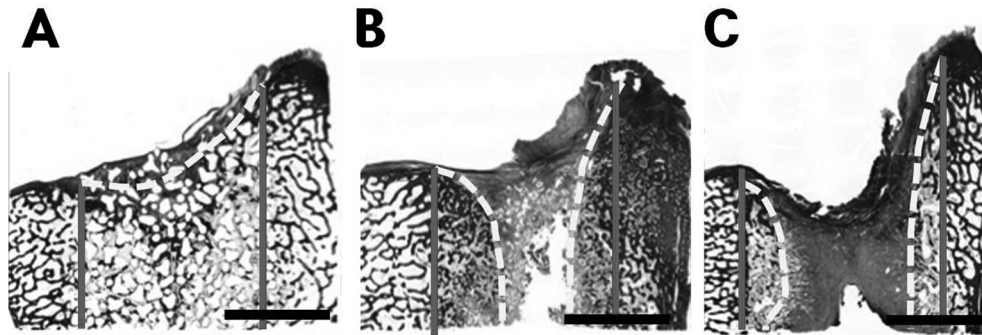between the β-TCP and control groups.

Fig. 7.   Histological findings of the 3 groups after 8 weeks of implantation. In the Tetrabones group, new bone
tissues were connected and almost filled all the intergranular spaces (A). In the β-TCP group, New bone tissues
and fibrous tissues were found in the defect (B). In the control group, a large amount of fibrous tissue was
found in the defect with empty space with scant new bone tissues (C). (solid line: the margin of the defect,
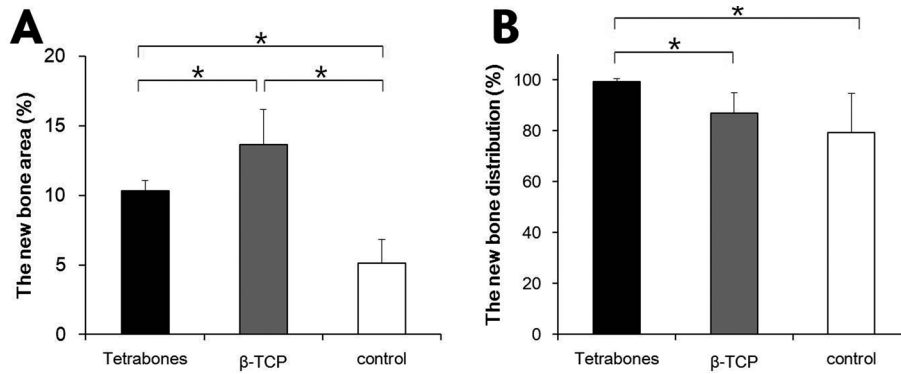dotted line: the inner margin of the new bone tissue; scale bar: 5 mm).

Fig. 8.   The new bone area (A) and distribution (B) of the 3 groups. New bone area of the β-TCP group
was significantly higher than those of the Tetrabone and control groups ($P<0.05$, A). However, the
distribution of new bone tissue was significantly higher in the Tetrabone group than those of the
β-TCP and control groups ($P<0.05$, B)

DISCUSSION

Various critical-size bone defect models have been reported in the skull, mandible and limb diaphyses of dogs [7, 14]. In this study, we created a large bone defect of 10 mm in diameter in the distal femoral condyles to evaluate the implantation effect of Tetrabones in critical sized defect. This cylindrical type defect could occur after collecting cancellous bone, the teeth extraction or removal of benign bone tumor in animals and treatments for osteochondorosis dissencanse or fibrous dysplasia in humans. None of the dogs used in this study showed lameness, even on the day after surgery. In the control group, the bone defect did not heal with minimal new bone tissue formation, suggesting that this model satisfies critical-size requirements and is adequate to analyze bone regeneration in dogs.

Superior biodegradability and osteoconductivity of β-TCP granules are well described [6, 12]. However, premature degradation of β-TCP granules could induce loss of osteoconductivity *in vivo* and result in insufficient bone re-

generation. Okanoue *et al*. reported that resorption of β-TCP granules was not necessarily accompanied by bone ingrowth in a rabbit bone defect model [13]. Generally, rodents have higher bone metabolic activity than other mammals, which can induce rapid granule degradation and new bone formation [17]. Therefore, we aimed to confirm the biodegradability of 2 types of granular artificial bone by using a canine bone defect model.

On CT and micro-CT analyses, β-TCP granules were rapidly degraded, resulting in a higher non-osseous tissue rate than that of Tetrabone®. This result may indicate that osteoconductivity of β-TCP granules is adversely affected by the rapid degradation of β-TCP. Nonconcurrent degradation and osteoconductivity in the β-TCP group might have induced the concave formation at the opening of the defect in the control group. Coupled with the size of the defect, the existence of non-osseous bone within the defect might have resulted in decreased mechanical strength *in situ* and the collapse of the defect.

On histology, the area of new bone tissue in the β-TCP

group was higher than that of the Tetrabone group. This result indicated that the granules may be transposed to new bone tissues, because of their superior biodegradability in the early stage of implantation. However, its area was restricted to the peripheral region of the defect and resulted in lower new bone distribution than that of Tetrabone group. The central region of the defect was filled with fibrous tissue in the β-TCP group. Similarly, other researchers reported that β-TCP granule implantation resulted in deficient bone tissue in the central region of the bone defect [16, 17]. Additional implantation of β-TCP granules may be required to repair the defect completely. As demonstrated in this study, the granules began to degrade and resulted in loss of their osteoconductivity before sufficient bone had formed. Yuan *et al.* reported that β-TCP alone could not repair canine mandibular bone defects [19]. In the meanwhile, Tetrabone group showed homogeneously distributed new bone tissues, although their area was lower than that of β-TCP group. Lower new bone tissue area may be induced by slower degradation of Tetrabones. However, slower biodegradability of Tetrabones could maintain their osteoconductivity and avoid forming fibrous tissues in the defect. This characteristic of Tetrabones may be advantageous for the critical sized bone defects, which need long period for complete repair. In addition, it could provide the biomechanical stability *in situ* [3].

The connectivity of the pores may primarily contribute to osteoconductivity *in vivo* [15, 18]. Although pore size of Tetrabone® and β-TCP granules is similar (100–500 μm), total porosity of β-TCP granules is greater than that of Tetrabone® [3]. However, connectivity of intergranular pores of a size appropriate for cell and blood vessel invasion is much higher in Tetrabone® than β-TCP granules, and this connective structure may facilitate migration of more osteogenic cells and blood vessels [3].

The difference in intergranular pores between the 2 types of granules may result from their size and shape. The β-TCP granules used in this study have heterogeneous sizes (0.5–1.5 mm). When they are accumulated, the smaller granules may locate between the larger granules, which may interrupt the connection of the intergranular pores. Furthermore, β-TCP granules are very fragile and may become compressed to less than 0.5 mm during implantation. Tetrabone® has homogeneous size and shape, thus creating more connected intergranular pores of less than 600 μm in size, which may induce clinically effective interconnective networks between the granules [3]. This highly connected porous structure might have enabled migration of osteogenic cells and blood vessels to the defect and complete distribution of new bone tissue inside the defect [3].

In this study, we observed the repair for 8 weeks of implantation. However, this experimental period might have been inadequate for early estimation of new bone tissue formation in the defect. The area and distribution of the new bone tissue can be changed with time, because bone remodeling process could have started at 8 weeks. In addition, degradation of calcium phosphate artificial bone depends on the implanted site, such as cortical, cancellous or medullar sites [11]. In the defect model used in this study, β-TCP granules might

have degraded rapidly, because the defect was surrounded by cancellous bone. A further study is needed to investigate the effects on bone formation in different implantation sites and for a longer period.

In conclusion, Tetrabone® showed homogeneous new bone tissue in large bone defects of dogs, while β-TCP granules resulted in heterogeneous new bone tissue with fibrous tissue formation at the central region of the defect. These differences may be caused by differences in biodegradability and interconnectivity of intergranular pores. Tetrabone® might be a superior artificial bone for repair of large bone defects of dogs in clinical practice.

REFERENCES

1. Baqain, Z. H., Anabtawi, M., Karaky, A. A. and Malkawi, Z. 2009. Morbidity from anterior iliac crest bone harvesting for secondary alveolar bone grafting: an outcome assessment study. *J. Oral Maxillofac. Surg.* **67**: 570–575. [Medline] [CrossRef]
2. Bucholz, R. W., Carlton, A. and Holmes, R. 1989. Interporous hydroxyapatite as a bone graft substitute in tibial plateau fractures. *Clin. Orthop. Relat. Res.* **240**: 53–62. [Medline]
3. Choi, S., Liu, I. L., Yamamoto, K., Igawa, K., Mochizuki, M., Sakai, T., Echigo, R., Honnami, M., Suzuki, S., Chung, U. I. and Sasaki, N. 2012. Development and evaluation of tetrapod-shaped granular artificial bones. *Acta Biomater.* **8**: 2340–2347. [Medline] [CrossRef]
4. Giannoudis, P. V., Dinopoulos, H. and Tsiridis, E. 2005. Bone substitutes: an update. *Injury* **36**: S20–S27. [Medline] [CrossRef]
5. Goto, T., Kojima, T., Iijima, T., Yokokura, S., Kawano, H., Yamamoto, A. and Matsuda, K. 2001. Resorption of synthetic porous hydroxyapatite and replacement by newly formed bone. *J. Orthop. Sci.* **6**: 444–447. [Medline] [CrossRef]
6. Hirota, M., Matsui, Y., Mizuki, N., Kishi, T., Watanuki, K., Ozawa, T., Fukui, T., Shoji, S., Adachi, M., Monden, Y., Iwai, T. and Tohnai, I. 2009. Combination with allogenic bone reduces early absorption of beta-tricalcium phosphate (beta-TCP) and enhances the role as a bone regeneration scaffold. Experimental animal study in rat mandibular bone defects. *Dent. Mater. J.* **28**: 153–161. [Medline] [CrossRef]
7. Horner, E. A., Kirkham, J., Wood, D., Curran, S., Smith, M., Thomson, B. and Yang, X. B. 2010. Long bone defect models for tissue engineering applications: criteria for choice. *Tissue Eng. Part B Rev.* **16**: 263–271. [Medline] [CrossRef]
8. Karageorgiou, V. and Kaplan, D. 2005. Porosity of 3D biomaterial scaffolds and osteogenesis. *Biomaterials* **26**: 5474–5491. [Medline] [CrossRef]
9. Kasten, P., Beyen, I., Niemeyer, P., Luginbuhl, R., Bohner, M. and Richter, W. 2008. Porosity and pore size of beta-tricalcium phosphate scaffold can influence protein production and osteogenic differentiation of human mesenchymal stem cells: an *in vitro* and *in vivo* study. *Acta Biomater.* **4**: 1904–1915. [Medline] [CrossRef]
10. LeGeros, R. Z. 2002. Properties of osteoconductive biomaterials: calcium phosphates. *Clin. Orthop. Relat. Res.* **395**: 81–98. [Medline] [CrossRef]

11. Lu, J. X., Gallur, A., Flautre, B., Anselme, K., Descamps, M., Thierry, B. and Hardouin, P. 1998. Comparative study of tissue reactions to calcium phosphate ceramics among cancellous, cortical, and medullar bone sites in rabbits. *J. Biomed. Mater. Res.* **42**: 357–367. [Medline] [CrossRef]

12. Luvizuto, E. R., Queiroz, T. P., Margonar, R., Panzarin, S. R., Hochuli-Vieira, E., Okamoto, T. and Okamoto, R. 2012. Osteoconductive properties of beta-tricalcium phosphate matrix, polylactic and polyglycolic acid gel, and calcium phosphate cement in bone defects. *J. Craniofac. Surg.* **23**: e430–e433. [Medline] [CrossRef]

13. Okanoue, Y., Ikeuchi, M., Takemasa, R., Tani, T., Matsumoto, T., Sakamoto, M. and Nakasu, M. 2012. Comparison of *in vivo* bioactivity and compressive strength of a novel superporous hydroxyapatite with beta-tricalcium phosphates. *Arch. Orthop. Trauma Surg.* **132**: 1603–1610. [Medline] [CrossRef]

14. Schmitz, J. P. and Hollinger, J. O. 1986. The critical size defect as an experimental model for craniomandibulofacial nonunions. *Clin. Orthop. Relat. Res.* **205**: 299–308. [Medline]

15. Tamai, N., Myoui, A., Tomita, T., Nakase, T., Tanaka, J., Ochi, T. and Yoshikawa, H. 2002. Novel hydroxyapatite ceramics with an interconnective porous structure exhibit superior osteoconduction *in vivo*. *J. Biomed. Mater. Res.* **59**: 110–117. [Medline] [CrossRef]

16. von Doernberg, M. C., von Rechenberg, B., Bohner, M., Grunenfelder, S., van Lenthe, G. H., Muller, R., Gasser, B., Mathys, R., Baroud, G. and Auer, J. 2006. *In vivo* behavior of calcium phosphate scaffolds with four different pore sizes. *Biomaterials* **27**: 5186–5198. [Medline] [CrossRef]

17. Wheeler, D. L., Cross, A. R., Eschbach, E. J., Rose, A. T., Gallogly, P. M., Lewis, D. D. and Vander Griend, R. A. 2005. Grafting of massive tibial subchondral bone defects in a caprine model using beta-tricalcium phosphate versus autograft. *J. Orthop. Trauma* **19**: 85–91. [Medline] [CrossRef]

18. Yoshikawa, H., Tamai, N., Murase, T. and Myoui, A. 2009. Interconnected porous hydroxyapatite ceramics for bone tissue engineering. *J. R. Soc. Interface* **6**: S341–S348. [Medline] [CrossRef]

19. Yuan, J., Cui, L., Zhang, W. J., Liu, W. and Cao, Y. 2007. Repair of canine mandibular bone defects with bone marrow stromal cells and porous beta-tricalcium phosphate. *Biomaterials* **28**: 1005–1013. [Medline] [CrossRef]